



Full Length Article

Development of Alginate-Montmorillonite-Starch with Encapsulated *Trichoderma harzianum* and Evaluation of Conidia Shelf Life

Fariz Adzmi^{1*}, Mohamed Hanafi Musa², Yasmeeen Siddiqui³, Wong Mui Yun³, Hazandy Abdul Hamid^{4,5}, Arifin Abdu⁵ and Rambod Abiri⁵

¹Laboratory of Plantation Science and Technology, Institute of Plantation Studies, Universiti Putra Malaysia, 43400 Serdang, Selangor, Malaysia

²Department of Land Management, Faculty of Agriculture, Universiti Putra Malaysia, 43400 Serdang, Selangor, Malaysia

³Laboratory of Sustainable Agronomy and Crop Protection, Institute of Plantation Studies, Universiti Putra Malaysia, 43400 Serdang, Selangor, Malaysia

⁴Laboratory of Bioresource Management, Institute of Tropical Forestry and Forest Product, Universiti Putra Malaysia, 43400 Serdang, Selangor, Malaysia

⁵Department of Forestry Science and Biodiversity, Faculty of Forestry and Environment, Universiti Putra Malaysia, 43400 Serdang, Selangor, Malaysia

*For correspondence: farizadzmi@upm.edu.my

Received 04 December 2020; Accepted 08 March 2021; Published 10 June 2021

Abstract

Biological control agents, such as *Trichoderma harzianum*, are widely used in sustainable agriculture. However, commercialisation and mass production of biocontrol products have remained a challenge, especially in viability and efficiency in field application. The encapsulation method has emerged as a sophisticated technique to develop the formulation of *T. harzianum*. Hence, encapsulation through extrusion was used to prepare *T. harzianum* beads. The physical characteristics comprising weight, diameter, and swelling ability of the beads were significantly improved when the starch percentage was increased. Alginate-montmorillonite-starch (10%) revealed the lowest shrinkage and the highest swelling ability. The interaction within the functional groups of alginate, montmorillonite, and starch was confirmed by the Fourier-transform infrared spectroscopic (FTIR) study. Furthermore, scanning electron microscopic analysis exposed compatible scattering of montmorillonite particles and starch granules over the alginate linkages. Meanwhile, the X-ray diffraction analysis confirmed the exfoliation between starch and montmorillonite. Storage of *T. harzianum* beads at 5°C was more suitable than storage at 28°C. At low temperature, the encapsulated *T. harzianum* beads maintained their viability at $6.59 \pm 0.12 \log \text{CFU g}^{-1}$ for an effective threshold value for up to seven months. The current findings indicated that the combination of alginate, montmorillonite, and starch is the best formulation of encapsulated *T. harzianum* with improved conidia shelf life. © 2021 Friends Science Publishers

Keywords: Alginate-montmorillonite-starch; Biological control agents; Encapsulation; Extrusion; Shelf life; *Trichoderma harzianum*

Introduction

Sustainable agriculture practices emphasise environmental friendliness to adopt new sustainable methods, such as using microorganisms as biological control agents (BCAs) to control plant pathogens (Curtis *et al.* 2010). The BCAs have emerged as one of the preferred management strategies to reducing yield loss and is innocuous to human beings (Lecomte *et al.* 2016). The biggest challenges for BCAs to be competitive in the market than chemical fungicides are consistency, effectiveness, and shelf life. These issues can be solved through scientific development in formulating BCAs (Kumar *et al.* 2019).

Encapsulation is emerging as a sophisticated technology for the formulation of BCAs. The advantages of encapsulation include significantly prolonged shelf life of BCAs by offering protection or stabilisation from biotic and abiotic stress factors, such as soil antagonists, contaminations, temperature, dryness, and ultraviolet (UV) light; or from mechanical stress by altering physical properties and providing a beneficial microenvironment (Rathore *et al.* 2013). This technology helps to maintain the metabolic activity of BCAs for an extended period during storage and after application (Szczech and Maciorowski 2016). Another important feature of encapsulation is the controlled release of the entrapped cells or spores (He *et al.*

2015), where they can be released by the factor of osmosis from the bead matrix or by the degradation of the encapsulation material. The released cells or spores can survive longer in the soil or with extended persistence, resulting in fewer applications and doses (Schoebitz *et al.* 2012; Ma *et al.* 2015). The choice of carrier for the encapsulation matrix is an important factor determining the success of BCA encapsulation.

Generally, biodegradable polymer materials, specifically natural polysaccharides such as alginate, gum, *k*-carrageenan, and agar, are used as a matrix (Vemmer and Patel 2013). Among these compounds, alginate is most preferred for carrier encapsulation. It is originally from brown seaweed that consists of linear unbranched polymers β -(1 \rightarrow 4)-linked D-mannuronic acid (M) and γ -(1 \rightarrow 4)-linked L-guluronic acid (G) residues (Tavassoli-Kafrani *et al.* 2016). The characteristics of alginate, such as biodegradability, nontoxicity, biocompatibility, and ease of gelation with various cross-linking agents, render it a preferred carrier material for BCAs (Tam *et al.* 2011; Simó *et al.* 2017). However, like other hydrogels, the limitations of alginate include mechanical stiffness, distorted shape, varying size, and poor physical properties that make it unsuitable for providing long-term stability of the encapsulated cells (Sriamornsak *et al.* 2017; Rodrigues *et al.* 2020).

Thus, to overcome these limitations, suitable filler is usually added to the formulation. It could be soluble, insoluble, or a combination of both. Fillers, such as montmorillonite and starch, were used to formulate encapsulated beads (Mohammadi *et al.* 2019). Montmorillonite is a three-layered mineral consisting of two tetrahedral layers sandwiched around a central octahedral layer (Itadani *et al.* 2017). It has several advantages, e.g., high cation exchange capacity, large surface area, excellent swelling ability, and is naturally present in soils, making montmorillonite a suitable filler encapsulation (Chevallard *et al.* 2012). Meanwhile, starch is a biodegradable polysaccharide, cheap and easily available (Riyajan 2017). The incorporation of fillers attracts great attention because of the noticeable improvements in the physical properties of the beads when loading is only between 1% and 3% (Fernandez-Perez *et al.* 2004). Moreover, fillers act as core substructure to curb shrinkage and result in the shape of the beads during the dehydration process (Singh *et al.* 2009).

Trichoderma harzianum has a wide spectrum of antimicrobial activity. Depending on the strain, *Trichoderma* is known to (i) colonise the rhizosphere (rhizosphere competence) and concede acceleration establishment in the substantial microbial environment around the rhizosphere; (ii) restrain plant pathogens through diverse mechanisms (Ali *et al.* 2020; Khan *et al.* 2021); (iii) enhance plant growth (Javaid *et al.* 2021); and (iv) control root growth (Soresh and Harman 2008). Generally, their efficacy in the field is restricted due to the factors above. Therefore, this study was performed to encapsulate *T. harzianum* in alginate, montmorillonite, and starch

formulation. The aims were to improve the physical properties and characterise chemical interaction of the materials used in the encapsulation formulation, and concurrently study the shelf life of the *T. harzianum* beads.

Materials and Methods

Encapsulation of *T. harzianum* in alginate-montmorillonite-starch beads

T. harzianum (UPMC 243) was obtained from the Microbial Culture Collection Unit at the Institute of Bioscience, Universiti Putra Malaysia. Twenty-five culture plates of *T. harzianum* were maintained on the potato dextrose agar (Becton, Dickinson and Company, USA) media at $28 \pm 2^\circ\text{C}$. To get the conidial pellet, 10 mL of sterile distilled water was added into each of the seven-day-old *T. harzianum* culture plates, and the surface was scraped gently with a sterilised bent glass rod. The conidial suspension was centrifuged at 7000 rpm for 10 min (Wijesinghe *et al.* 2011), and the beads were prepared using the extrusion technique (Raha *et al.* 2018). Accordingly, 2.5 g (1% w/v) of montmorillonite (K 10, Sigma-Aldrich) and 2.5 g (1% w/v) of starch (Becton, Dickinson and Company, U.S.A.) were dispersed together in 250 mL sterile distilled water and stirred for 24 h to form a homogenous solution. Then, 5 g (2% w/v) of alginate powder (Sigma-Aldrich) was added to the starch and montmorillonite solution and stirred for 2 h using a magnetic stirrer (Heidolph, Germany). Subsequently, *T. harzianum* conidial pellets were added to the mixture with continuous stirring for another 4 h to give a conidial concentration of $1.3 \times 10^{11} \text{ mL}^{-1}$. Finally, the mixture was dropped through a 10 mL pipette tip from a 15 cm height into 0.5 M CaCl_2 (Sigma-Aldrich) under constant stirring for gelation. After 2 h, the beads were taken out of the CaCl_2 solution by sieving and washed several times with distilled water. The beads were then allowed to dry at room temperature for 24 h. The experiment was performed in a similar manner using 3%, 5%, and 10% (w/v) of starch, with a fixed amount of 2% alginate and 1% montmorillonite (Bokkhim *et al.* 2016).

Physical characterisation

In total, 20 beads were measured, with five beads sampled randomly from each treatment (varying concentrations of starch). The weight of the beads was measured using a digital balance (Mettler Toledo, Switzerland) and expressed in milligrams (mg). The diameter of the beads was measured using a stereomicroscope (Leica Microsystems, Germany), and the bead shape was calculated using a sphericity factor (SF) (Chan *et al.* 2011a):

$$SF = \left(\frac{d_{\max} - d_{\min}}{d_{\max} + d_{\min}} \right) \times 100 \quad (1)$$

Where, d_{\max} is the largest diameter and d_{\min} is the smallest diameter of the beads.

Shrinkage of encapsulated beads was determined using the following equation:

$$\text{Shrinkage (\%)} = \left(\frac{D_w - D_d}{D_w} \right) \times 100 \quad (2)$$

Where, D_w is the diameter of the wet beads and D_d is the diameter of the dry beads.

The swelling capacity or ability of the encapsulated beads was measured by suspending 20 dried beads from each concentration of starch in 10 mL of distilled water with five replicates under mild shaking for 24 h. The swollen beads were removed and pressed between two filter papers to remove the excess water and weighed on a digital balance. The swelling percentage was calculated using the following equation (Dai *et al.* 2019):

$$\text{Swelling (\%)} = \frac{(W_s - W_d)}{W_d} \times 100 \quad (3)$$

Where, W_s and W_d are the weights of the swollen and dry beads, respectively.

Chemical characterisation

Alginate-montmorillonite-starch (10%) was chosen for chemical characterisation. The assessment was conducted using an FTIR spectrophotometer (Perkin Elmer 1650, U.S.A) *via* the KBr disc method. Each sample was pulverised, gently triturated with KBr powder at a weight ratio of 1:100, and then pressed using a hydrostatic press at 10 tons for 5 min. The disc was placed in the sample holder and scanned from 4000 to 400 cm^{-1} at a resolution of 4 cm^{-1} . The internal morphology of the encapsulated beads was analysed using a scanning electron microscope (SEM; JEOL, U.S.A. and Leo 1455, Germany) at 1000 \times magnification. The X-ray diffraction (XRD) analysis was recorded using an XRD diffractometer (Siemens D-5000, U.S.A.) with Cu K α ($\lambda = 1.5418 \text{ \AA}$) radiation at 40 kV and 40 mA (Pawar *et al.* 2018).

Entrapment efficacy, conidia release, and stability of *T. harzianum* beads

A total of ten individual *T. harzianum* beads were taken from each starch concentration. The beads were mashed using a sterile mortar and pestle. An amount of 10 mL sterile distilled water was added to the resulting powder from the encapsulated beads. Serial dilutions were made, and 0.1 mL aliquots were plated on rose Bengal agar media, where all plates were incubated at $28 \pm 2^\circ\text{C}$. The number of colonies formed after four days of incubation was recorded as colony-forming units (CFU) per encapsulated bead. The plate count was conducted in five replicates, where the average was considered the final value of CFU per *T. harzianum* encapsulated beads.

Conidial release of *T. harzianum* encapsulated beads over time were determined by suspending 100 mg of *T. harzianum* beads in 10 mL sterile distilled water followed

by incubation for 2 h with mild agitation at 160 rpm. Serial dilutions of the suspension were made, and 0.1 mL aliquots were plated on a rose Bengal medium, followed by incubation at $28 \pm 2^\circ\text{C}$. The number of colonies formed after four days of incubation was recorded as CFU g^{-1} and expressed as log CFU g^{-1} of encapsulated beads. The plate count was conducted in five replicates. The final value of CFU g^{-1} *T. harzianum* was the average of the five readings. The experiment was repeated at different incubation times of 4, 8, 12, 24, and 48 h. The stability of *T. harzianum* in the encapsulated formulation was determined *via* a similar procedure of conidia release. The incubation time was 24 h, and measurements were made at monthly intervals throughout the 12-month storage period.

Statistical analysis

The data were analysed using a one-way analysis of variance (ANOVA) with Statistical Analysis Software (S.A.S.) 9.2. The effect of the treatment was considered significant at $P \leq 0.05$. Statistical analyses of *t*-test and *f*-test were applied to determine the significance of the treatment, while the mean comparison was performed according to the least significant difference (LSD) method.





Results

Physical characterisation of the alginate-montmorillonite-starch

The physical appearance of the beads prepared with different concentrations of starch as filler in alginate-montmorillonite-starch combination is tabulated in Table 1. Significant differences ($P \leq 0.05$) in weight and diameter of encapsulated beads and positive correlation ($R^2 = 0.95$) were observed with the increased amount of starch from 1% to 10%. The weight increased from 2.79 ± 0.10 to 7.27 ± 0.25 mg, while the diameter increased from 1.39 ± 0.06 to 1.94 ± 0.03 mm (Table 1). The sphericity factor (SF) was used to determine the shape of the beads because it can accurately detect the change of the beads. The SF varied from zero (for a perfect sphere) to one (for an elongated structure). Table 1 shows the SF of beads in the range of 0.03 ± 0.002 to 0.07 ± 0.009 , indicating that most of the beads are spherical. The best spherical shape is noted in beads with 10% starch modification.

Similarly, significant differences ($P \leq 0.05$) in beads shrinkage are noted between alginate-montmorillonite-starch (1%), alginate-montmorillonite-starch (3%), and alginate-montmorillonite-starch (10%) (Table 1). Increasing the starch concentration will affect the shrinkage characteristic, where the level of shrinkage is reduced by 25%. In comparison, the bead swelling for the starch concentration at 1%, 3%, and 5% did not exhibit any statistical differences ($P \leq 0.05$). However, alginate-montmorillonite-starch (10%) showed a significant

Table 1: Comparison of physical appearance, weight, diameter, shrinkage, shape factor, and swelling ability of alginate–montmorillonite–starch beads with varied starch concentrations

Starch content (%)	1	3	5	10
Physical appearance				
Weight (mg)	2.79 ± 0.1 ^d	3.99 ± 0.04 ^c	4.47 ± 0.06 ^b	7.27 ± 0.25 ^a
Diameter (mm)	1.39 ± 0.06 ^d	1.60 ± 0.04 ^c	1.74 ± 0.02 ^b	1.94 ± 0.03 ^a
Shrinkage (%)	58.31 ± 1.82 ^a	47.98 ± 1.37 ^b	48.48 ± 0.55 ^b	43.30 ± 1.38 ^c
Sphericity factor	0.07 ± 0.009 ^a	0.62 ± 0.014 ^{ab}	0.41 ± 0.002 ^b	0.39 ± 0.002 ^b
Swelling (%)	59.31 ± 5.64 ^b	60.05 ± 2.02 ^b	62.11 ± 0.97 ^b	67.31 ± 1.9 ^a

Values show the means ± standard error (n = 5). Data with different letters (a–d) in a row are significantly different at $P \leq 0.05$ using LSD

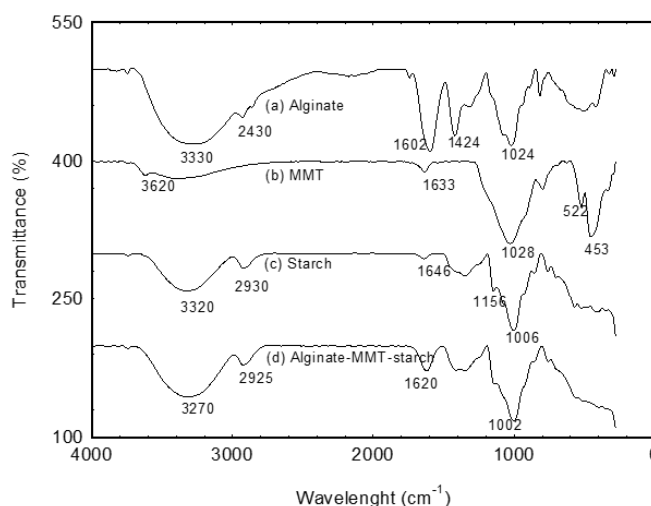


Fig. 1: FTIR spectrum of (a) alginate; (b) montmorillonite; (c) starch and (d) alginate- montmorillonite-starch. The shifting characteristic peaks of alginate and starch in the alginate- montmorillonite-starch confirm the interaction between functional groups

difference ($P \leq 0.05$) than other treatments, with the swelling ability increasing by approximately 8% (Table 1).

Chemical characterisation of alginate-montmorillonite-starch

The FTIR study revealed a broad band spectrum for all samples in the region between 3270 and 3330 cm^{-1} attributed to the O–H stretching of water molecules. Alginate characteristic peaks at bands 1602 and 1424 cm^{-1} refer to the asymmetric and symmetric COO^- stretching, while the peak at 1024 cm^{-1} is attributed to the C–O–C stretching (Fig. 1). The characteristic montmorillonite peaks observed at 3620 cm^{-1} is attributed to the Si–OH stretching, while the following peak at 1633 cm^{-1} is of the OH bending of water molecules. The peak observed at 1028 cm^{-1} is attributed to the Si–O–Si stretching, while the Si–O bending vibrations are seen at 522 and 453 cm^{-1} . The characteristic peak for starch observed at 2930 cm^{-1} is attributed to the C–H stretching. Meanwhile, the peaks observed at 1156 and 1006 cm^{-1} represent the C–O and C–C stretching of the starch polymer glucose unit.

The internal morphological structure of alginate has a uniform interpenetrating alginate linkage, which is dense and packed (Fig. 2a). Montmorillonite has an irregular plate-like pattern of hundreds of micrometres in two-dimension, length, and width (Fig. 2b), while starch shows round polygonal shapes sized at 12.93 μm (Fig. 2c). The surface area of starch is 0.014 m^2g^{-1} , with a pore diameter of 2588 Å, while the montmorillonite surface area is 227.56 m^2g^{-1} , with a pore diameter of 60.68 Å. Although no surface area was recorded for alginate due to the hydrogel linkage, it has a pore diameter of 175.24 Å. The morphology of alginate-montmorillonite-starch beads showed a homogenous distribution of starch particles in the matrix (Fig. 2d), with the surface area and pore diameter of 4.462 m^2g^{-1} and 43.27 Å.

The X-ray diffraction analyses of alginate, montmorillonite, starch, and alginate-montmorillonite-starch are shown in Fig. 3. The characteristic sharp peak of montmorillonite at 2θ of 8.8° corresponded to a d -spacing value of 5.04 Å. The interlayer spacing of the montmorillonite structure is in the diffraction range between 2° and 10°. Meanwhile, the d -spacing value of starch is 2.96

Table 2: Comparison of entrapped *T. harzianum* conidia in alginate–montmorillonite–starch beads with different concentration of starch before and after drying process

Alginate (% w/v)	Montmorillonite (% w/v)	Starch (% w/v)	Before drying (log CFU g ⁻¹)	After drying (log CFU g ⁻¹)
2	1	1	5.49 ± 0.06 ^{dA}	4.42 ± 0.27 ^{bB}
2	1	3	5.86 ± 0.04 ^{cA}	4.64 ± 0.16 ^{bB}
2	1	5	6.18 ± 0.06 ^{bA}	5.36 ± 0.03 ^{aB}
2	1	10	6.35 ± 0.05 ^{aA}	5.42 ± 0.20 ^{aB}

Value (s) are presented as means ± standard error (n = 5). Values with different letters are significant at $P \leq 0.05$. Capital letters (A-B) correspond to the values for different treatments (within column). Small letters (a-d) correspond to the values for different treatments (within row)

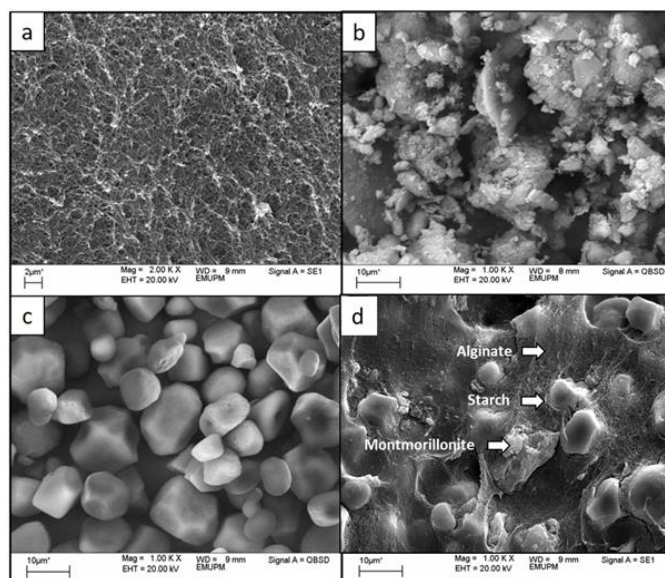


Fig. 2: SEM images of the cross sections of: (a) homogenous interpenetrating of alginate network; (b) irregular plate-like of montmorillonite; (c) starch granules polygonal; and (d) homogenous distribution of montmorillonite and starch in the alginate linkage network of the alginate-montmorillonite-starch beads

Å at 2θ of 15.06° . No peak was observed for alginate, confirming that alginate has an amorphous structure. The intensity of the characteristic peak at 2θ of 17.48° for starch decreased at 2θ of 17.56° for the alginate-montmorillonite-starch mixture. Simultaneously, the intensity peak for montmorillonite at 2θ of 20.61° decreased in alginate-montmorillonite-starch at 2θ of 26.80° .

Viability and stability of encapsulated *T. harzianum* beads

The initial concentration of *T. harzianum* conidia in the suspension was 1.3×10^{11} CFU mL⁻¹. Significant differences ($P \leq 0.05$) are observed between the concentrations of entrapped conidia of fresh beads when the starch percentage increases from 1% to 10% (Table 2). Conidia entrapped in fresh beads increased from 5.49 ± 0.06 to 6.35 ± 0.05 log CFU g⁻¹, and for dry beads, though lower than the fresh beads, they still increased from 4.42 ± 0.06 to 5.42 ± 0.06 log CFU g⁻¹, with increasing concentration of starch.

The SEM image of the cross-section of trapped *T. harzianum* in encapsulated beads (Fig. 4) shows the distribution of *T. harzianum* conidia throughout the matrix, whereby the average size of conidia is $2.59 \mu\text{m}$. Conidial

release of encapsulated *T. harzianum* beads as a function of time at a different percentage of starch content is elucidated in Fig. 5. No significant difference ($P \leq 0.05$) is noted in conidia release with increased starch concentration. The maximum release of conidia from alginate-montmorillonite-starch beads is 9.2 log CFU g⁻¹ at 10% starch concentration. However, the release is increased with time. Positive correlations ($R^2 = 0.84\text{--}0.86$) are observed between conidia release and time, irrespective of starch percentage (Fig. 5). Next, the viability of encapsulated *T. harzianum* in alginate-montmorillonite-starch (10%) in different storage conditions is shown in Fig. 6. The initial CFU is recorded at 8.37 ± 0.08 log CFU g⁻¹. The results revealed significant variation ($P \leq 0.05$) in the viability of *T. harzianum* encapsulated beads at low temperature than those stored at room temperature. At room temperature ($28^\circ\text{C} \pm 2^\circ\text{C}$), the viability of *T. harzianum* gradually decreased from 7.58 ± 0.15 to 6.81 ± 0.27 log CFU g⁻¹ within the first three months and further decreased to 3.23 ± 0.39 log CFU g⁻¹ in the fourth month. No recovery of *T. harzianum* is noted from the fifth month onwards. On the other hand, the viability of *T. harzianum* beads stored at a cold temperature (5°C) showed a slow and steady decline in CFU throughout the 12-month storage. The viable count ranged between 8.27 ± 0.18 and 1.55 ± 0.1 log

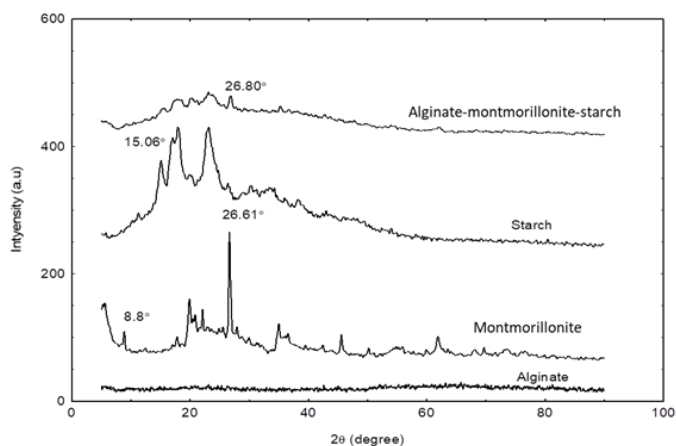


Fig. 3: XRD of alginate, montmorillonite, starch, and alginate–montmorillonite–starch

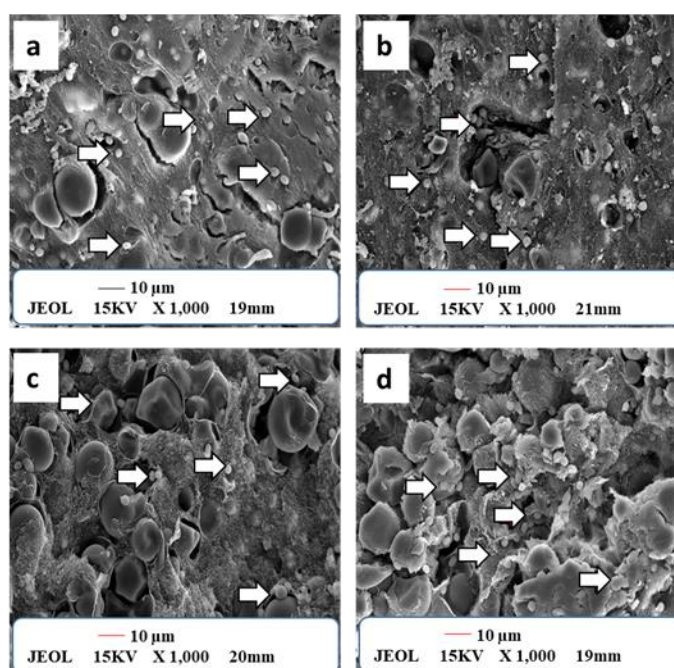


Fig. 4: SEM of the cross-section *T. harzianum* beads varied by different percentage of starch content; **a)** 1% starch; **b)** 3% starch; **c)** 5% starch; and **d)** 10% starch. Arrow showing the distribution of *T. harzianum* conidia throughout the alginate-montmorillonite-starch matrix

CFU g^{-1} . Thus, at low temperature, *T. harzianum* beads can be stored up to seven months, with an effective threshold value of $6.59 \pm 0.12 \log \text{CFU } g^{-1}$.

Discussion

In this study, *T. harzianum* was successfully encapsulated in the formulation of alginate, montmorillonite, and starch combination. The formulation was developed with a fixed amount of alginate (2%) and montmorillonite (1%) but a varied percentage of starch (1% to 10%). The physical appearance of the beads produced for all formulations was uniform with a smooth surface. This could be due to the releasing factors of BCAs, as reported in a previous study,

where the smooth surface facilitated the permeation of water into the bead matrix, releasing BCAs (Mithilesh and Ree 2012). The increased percentage of starch decreased the percentage of shrinkage. The reduction led to the assumption that the bigger the average sizes of the starch granule, the lower the total shrinkage percentage (Ramdhan *et al.* 2020). The swelling ability of the beads is an important factor in releasing entrapped conidia. In this study, the swelling ability was increased upon increased starch percentage. These findings could be explained by the initial increase in swelling due to the hydrophilicity of starch, which increased the hydrophilic nature of the beads' chemical formulation (Fernandes *et al.* 2019). Bead swelling is directly related to the osmotic pressure that

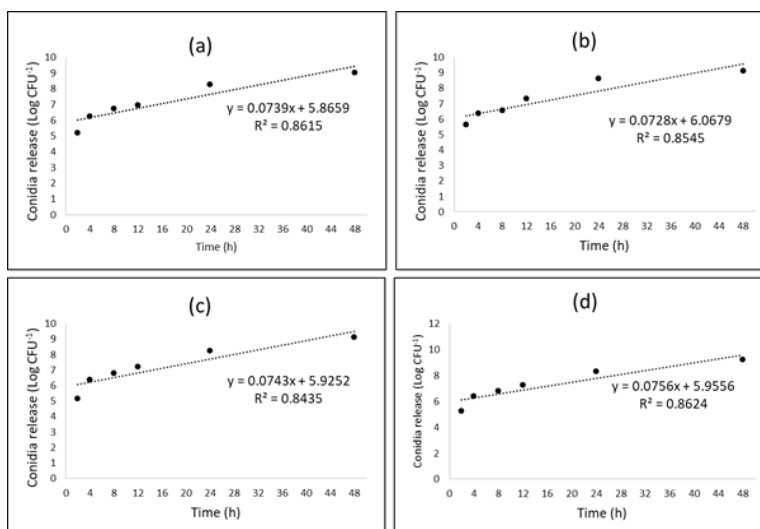


Fig. 5: Conidia release of encapsulated *T. harzianum* beads as function of time at different percentage of starch content: **a)** 1% starch; **b)** 3% starch; **c)** 5% starch; and **d)** 10% starch

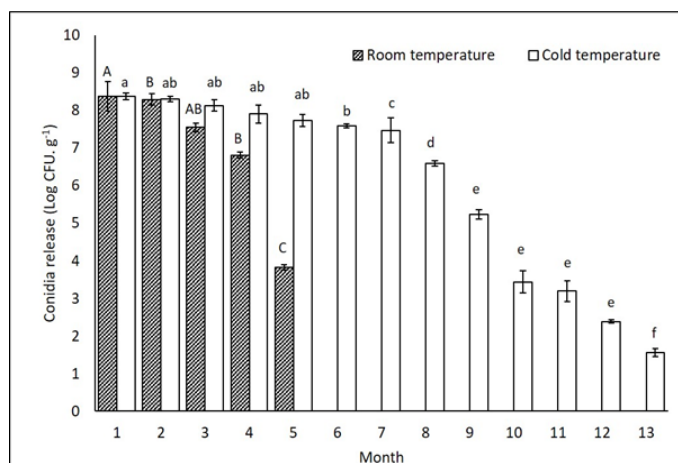


Fig. 6: Comparison between the viability of *T. harzianum* released from the encapsulated beads under different storage conditions (room temperature [28°C ± 2°C] and cold temperature [5°C ± 2°C]) throughout the 12 months storage. Bars indicate standard error and values are mean of five replicates (n = 5). (A-C) correspond to the values for cold storage conditions for the time intervals while (a-f) correspond to the values for room storage conditions for the time intervals

occurs by the degree of water absorption. The beads' swelling ratio can be controlled by adjusting their chemical composition (Roy *et al.* 2009). It was established that adding starch into the formulation could enhance the swelling capacity of the bead. The addition of starch to the matrix as filler enhances the bead swelling ability, which is advantageous for the controlled release of the active agent when the polymer system meets a compatible solvent or fluid in the environment (Wu *et al.* 2014). Controlled release formulations are better than rapid release formulations because they do not require multiple applications and can reduce the production cost while improving the microbial viability for effective disease control (Caldwell *et al.* 2012).

Chemical characterisation *via* FTIR for the alginate-

montmorillonite-starch formulation showed the interaction between the functional groups, *i.e.*, the shift of the peak characteristic of COO⁻ stretching for alginate from 1602 to 1620 cm⁻¹. This result indicates that the electrostatic interaction of the carbonyl group reduced the interaction of hydrogen bonding. Concurrently, stronger ionic interaction between carboxylate ions caused free delocalisation of electrons (Asadi-Korayem *et al.* 2021). Meanwhile, the peak for the Si-OH group of montmorillonites at 522 cm⁻¹ disappeared. The findings revealed the interaction of montmorillonite in the alginate-montmorillonite-starch, represented by the formation of hydrogen bonding between the silanol groups on the surface of montmorillonite (He *et al.* 2019). The interaction from starch in the alginate-montmorillonite-starch bead was observed by the shift in the

characteristic peak of C–H stretching from 2930 to 2924 cm^{-1} and C–O–C stretching from 1006 to 1002 cm^{-1} (Fig. 1). The interaction, which was also revealed on the XRD analysis, indicated that exfoliation occurred when the starch molecules and montmorillonite particles had dispersed in the alginate hydrogel networks (Almasi *et al.* 2010).

This study also revealed that fewer conidia were entrapped in the dried beads than the fresh ones. The difference between the entrapped conidia before and after drying, could be attributed to the decreased shrinkage percentage of the beads, as portrayed in this study. A high shrinkage percentage would have caused more physical stress to the conidia during the drying process. The montmorillonite particles would have been involved in building up the matrix to prevent the loss of *T. harzianum* conidia. The addition of starch filler may have caused the beads' internal structure to become more porous due to the distribution of the microparticles that occupied the spaces between the alginate and the montmorillonite (Thakur *et al.* 2016). Simultaneously, starch offers physical protection alteration in the beads matrix by shielding entrapped conidia released during the drying process (Zohar-Perez *et al.* 2004).

It was reported that the formulation of BCAs required conidia release from the beads to be conducted in a controlled and sustained manner to survive longer in the environment (Campos *et al.* 2014). The release mechanism of encapsulated conidia involved two processes; i) the penetration of molecules water into the beads matrix, followed by ii) the swelling of the beads caused by different osmotic pressure inside and outside (Jurić *et al.* 2019). Several studies reported that the storage condition has a significant impact on the viability and stability of encapsulated cells (Locatelli *et al.* 2008). The viability of 6.00 log CFU g^{-1} is considered as the limit for biological control agent to remain effective (Larena *et al.* 2003). This study found that low-temperature storage provided better stability of the encapsulated *T. harzianum* beads. The number of viability conidia maintained at 10^6 CFU g^{-1} after 7 months of storage at 4°C. At low temperature, various chemical reactions are suppressed, and the metabolic activity of the encapsulated *T. harzianum* may occur at a lower rate. In contrast, room temperature storage (28°C \pm 2°C) may expose the encapsulated *T. harzianum* to stress tolerance responses (Martin *et al.* 2013). The high-temperature storage showed lower cell stability, which could be due to various biochemical reactions, such as lipid oxidation and accelerated enzymatic reactions (Li *et al.* 2019). Moreover, oxygen was speculated to cause oxidation reactions, which could cause protein denaturation and phospholipid degradation of the dried biological materials (Przyklenk *et al.* 2017). Incorporating starch into the formulation will produce less porous and less hygroscopic beads, resulting in higher viability and stability upon the storage period (Chan *et al.* 2011b).

Conclusion

The combination of starch and montmorillonite as a filler changed the physical properties of the beads. FTIR analysis showed strong interactions between the functional groups of alginates, montmorillonite, and starch. The XRD analysis revealed the exfoliation of starch and montmorillonite in alginate hydrogel. The SEM analysis showed the homogenous distribution of the polygonal particles of starch throughout the alginate-montmorillonite-starch matrix. The *T. harzianum* beads could maintain the viability of 10^6 log CFU g^{-1} up to 7 months when stored at 5°C. Overall, the current study proposes the use of a combination of alginate, montmorillonite, and starch as a suitable matrix to encapsulate *T. harzianum*, suggesting a novel means of formulating BCAs. This encapsulation technique can be used for the storage, delivery, and practical applications of other BCAs.

Acknowledgements

This research was supported by a grant from the Ministry of Energy, Science, Technology, Environment and Climate Change Malaysia and was administered through Research and Development MESTECC Grant (02-01-04-SF2441).

Author Contributions

FA was involved in designing the work, drafting, writing, analysis, and interpretation of data. MHM, WMY, HAH, AA and RA contributed by interpreting the data, while YS contributed by planning the experiment and statistical analyses.

Conflict of Interest

The authors declare that they have no conflict of interest.

Data Availability

The data will be made available on acceptable request to the corresponding author.

Ethics Approval

No human and/or animal were used as research subject during this study.

References

- Ali A, A Javaid, A Shoaib, IH Khan (2020). Effect of soil amendment with *Chenopodium album* dry biomass and two *Trichoderma* species on growth of chickpea var. Noor 2009 in *Sclerotium rolfsii* contaminated soil. *Egypt J Biol Pest Cont* 30:1-9
- Almasi H, B Ghanbarzadeh, AA Entezami (2010). Physicochemical properties of starch–CMC–nanoclay biodegradable films. *Intl J Biol Macromol* 46:1–5

- Asadi-Korayem M, M Akbari-Taemeh, F Mohammadian-Sabet, A Shayesteh, H Daemi (2021). How does counter-cation substitution influence inter- and intramolecular hydrogen bonding and electrospinn ability of alginates. *Intl J Biol Macromol* 171:234–241
- Bokkhim H, N Bansal, L Grøndahl, B Bhandari (2016). Characterization of alginate–lactoferrin beads prepared by extrusion gelation method. *Food Hydrocoll* 53:270–276
- Caldwell CJ, RK Hynes, SM Boyetchko, DR Korber (2012). Colonization and bioherbicidal activity on green foxtail by *Pseudomonas fluorescens* BRG100 in a pesta formulation. *Can J Microbiol* 58:1–9
- Campos EVR, JLD Oliveira, LF Fraceto (2014). Applications of controlled release systems for fungicides, herbicides, acaricides, nutrients, and plant growth hormones: a review. *Adv Sci Eng Med* 6:373–387
- Chan ES, SL Wong, PP Lee, JS Lee, TB Ti, Z Zhang, D Poncelet, P Ravindra, SH Phan, ZH Yim (2011a). Effects of starch filler on the physical properties of lyophilised calcium-alginate beads and the viability of encapsulated cells. *Carbohydr Polym* 83:225–232
- Chan ES, TK Lim, WP Voo, R Pogaku, BT Tey, Z Zhang (2011b). Effect of formulation of alginate beads on their mechanical behaviour and stiffness. *Particuology* 9:228–234
- Chevillard A, H Angellier-Coussy, V Guillard, N Gontard, E Gastaldi (2012). Controlling pesticide release via structuring agropolymer and nanoclays based materials. *J Hazard Mater* 250:32–39
- Curtis FD, G Lima, D Vitullo, VD Cicco (2010). Biocontrol of *Rhizoctonia solani* and *Sclerotium rolfsii* on tomato by delivering antagonistic bacteria through a drip irrigation system. *Crop Prot* 29:663–670
- Dai A, Y Liu, B Ju, Y Tian (2019). Preparation of thermoresponsive alginate/starch ether composite hydrogel and its application to the removal of Cu (II) from aqueous solution. *Bioresour Technol* 294: Article 122192
- Fernandes RS, FN Tanaka, MRD Moura, MF Aouada (2019). Development of alginate/starch-based hydrogels crosslinked with different ions: Hydrophilic, kinetic and spectroscopic properties. *Mater Today Commun* 21: Article 100636
- Fernandez-Perez M, F Flores-céspedes, E Gonzáles-Pradas, M Villafranca-Sánchez, S Pérez-García, FJ Garido-Harrera (2004). Use of activated bentonites in controlled release formulation of atrazine. *J Agric Food Chem* 52:3888–3893
- He F, Q Zhou, L Wang, G Yu, J Li, Y Feng (2019). Fabrication of a sustained release delivery system for pesticides using interpenetrating polyacrylamide/alginate/montmorillonite nanocomposites hydrogels. *Appl Clay Sci* 183: 105347
- He Y, Z Wu, L Tu, G Zhang, C Li (2015). Encapsulation and characterization of slow release microbial fertilizer from the composite of bentonite and alginate. *Appl Clay Sci* 109–110:68–75
- Itadani A, M Tanaka, T Abe, H Taguchi, M Nagao (2007). Al-pillared montmorillonite clay minerals: Low-pressure CO adsorption at room temperature. *J Colloid Interf Sci* 313:747–750
- Javaid A, A Ali, A Shoaib, IH Khan (2021). Alleviating stress of *Sclerotium rolfsii* on growth of chickpea var. Bhakkar-2011 by *Trichoderma harzianum* and *T. viride*. *J Anim Plant Sci* 31:(In press)
- Jurić S, E Đermić, S Topolovec-Pintarić, M Bedek, M Vinceković (2019). Physicochemical properties and release characteristics of calcium alginate microspheres loaded with *Trichoderma viride* spores. *J Integr Agric* 18:2534–2548
- Khan IH, A Javaid, D Ahmed (2021). *Trichoderma viride* controls *Macrophomina phaseolina* through its DNA disintegration and production of antifungal compounds. *Intl J Agric Biol* 25:888–894
- Kumar S, M Nehra, N Dilbaghi, G Marrazza, AA Hassan, KH Kim (2019). Nano-based smart pesticide formulation: emerging opportunities for agriculture. *J Cont Rel* 294:131–153
- Larena I, P Sabuquillo, P Melgarejo, AD Cal (2003). Biocontrol of *Fusarium* and *Verticillium* wilt of tomato by *Penicilliumoxalicum* under greenhouse and field conditions. *J Phytopathol* 151:507–512
- Lecomte C, C Alabouvette, V Edel-Hermann, F Robert, C Steinberg (2016). Biological control of ornamental plant disease caused by *Fusarium oxysporum*: A review. *Biol Cont* 101: 17–30
- Li W, L Liu, H Tian, X Luo, S Liu (2019). Encapsulation of *Lactobacillus plantarum* in cellulose based microgel with controlled release behaviour and increase long-term storage stability. *Carbohydr Polym* 223: Article 115065
- Locatelli GO, GFD Santos, PS Botelho, CCL Finkler, LA Bueno (2018). Development of *Trichoderma* sp. Formulation in encapsulated granules (CG) and evaluation of conidia shelf-life. *Biol Contr* 117:21–29
- Ma X, X Wang, J Chen, XN Xuexin, YY Zhao, W Wang (2015). Microencapsulation of *Bacillus subtilis* B99-2 and its biocontrol efficiency against *Rhizoctonia solani* in tomato. *Biol Cont* 90:34–41
- Martin MJ, F Lara-Villoslada, MA Ruiz, ME Morales (2013). Effect of unmodified starch on viability of alginate-encapsulated *Lactobacillusfermentum* CECT5716. *LWT Food Sci Technol* 53:480–486
- Mithilesh Y, KY Rhee (2012). Superabsorbent nanocomposites (alginate-g-PAMPS/MMT): Synthesis, characterization and swelling behaviour. *Carbohydr Polym* 90:165–173
- Mohammadi M, MK Heshmadi, K Sarabandi, M Fathi, LT Lim (2019). Hamishehkar, H. Activated alginate-montmorillonite beads as an efficient carrier for pectinase immobilization. *Intl J Biol Macromol* 137:253–260
- Pawar RR, P Lalhmunsiam, SY Gupta, B Sawant, SM Shahmoradi, SM Lee (2018). Porous synthetic hectorite clay-alginate composite beads for effective adsorption of methylene blue dye from aqueous solution. *Intl J Biol Macromol* 114:1315–1324
- Przyklenk M, M Vemmer, M Hanitzsch, A Patel (2017). A bioencapsulation and drying method increases shelf life and efficacy of *Metarhizium brunneum* conidia. *J Microencapsul* 34:498–512
- Raha A, S Bhattacharjee, P Mukherjee, M Paul, A Bagchi (2018). Design and characterization of ibuprofen loaded alginate microspheres prepared by ionic gelation method. *Intl J Pharm* 6:2713–2716
- Ramadhan T, SH Ching, S Prakash, B Bhandari (2020). Physical and mechanical properties of alginate based composite gels. *Trends Food Sci Technol* 106:150–159
- Rathore S, PM Desai, CV Liew, LW Chan, DWS Heng (2013). Microencapsulation of microbial cells. *J Food Eng* 116:369–381
- Riyajan SD (2017). Physical property testing of a novel hybrid natural rubber-graft- cassava starch/sodium alginate bead for encapsulating herbicide. *Polym Test* 58:300–307
- Rodrigues FJ, MF Cedran, JL Bicas, HH Sato (2020). Encapsulated probiotic cells: Relevant techniques, natural sources as encapsulating materials and food applications – A narrative review. *Food Res Intl* 137:1-16
- Roy A, J Bajpai, AK Bajpai (2009). Dynamics of controlled release of chlorpyrifos from swelling and eroding biopolymeric microspheres of calcium alginate and starch. *Carbohydr Polym* 76:222–231
- Schoebitz M, H Simonin, D Poncelet (2012). Starch filler and osmoprotectant improve the survival of rhizobacteria in dried alginate beads. *J Microencapsul* 29:532–538
- Simó G, E Fernández- Fernández, J Villa-Crespo, V Ruipérez, JM Rodríguez-Nagolas (2017). Research progress in coating techniques of alginate gel polymer for cell encapsulation. *Carbohydr Polym* 170:1–14
- Singh B, DK Sharma, R Kumar, A Gupta (2009). Controlled release of the fungicide tiram from alginate-starch-clay based formulation. *Appl Clay Sci* 45:76–82
- Soresh M, GE Harman (2008). The relationship between increased growth and resistance induced in plants by root colonizing microbes. *Plant Signal Behav* 3:237–239
- Sriamomsak P, J Nanthanid, M Luangtana-anan, S Puttipipatkachorn (2017). Alginate-based pellets prepared by extrusion/spheronization: A preliminary study on the effect of additive in granulating liquid. *Eur J Pharm Biopharm* 67:227–235
- Szczeczek M, R Maciorowski (2016). Microencapsulation technique with organic additives for biocontrol agents. *J Hort Res* 24:111–112
- Tam SK, J Dusseault, S Bilodeau, JP Langlois (2011). Yahlia, L. Factors influencing alginate gel biocompatibility. *J Biomed Mater Res A* 98:40–52

- Tavassoli-Kafrani E, H Shekarchizadeh, M Masoudpour-Behabadi (2016). Development of edible films and coatings from alginates and carrageenans. *Carbohydr Polym* 137:360–374
- Thakur S, S Pandey, OA Arotiba (2016). Development of sodium alginate-based organic/inorganic superabsorbent composite hydrogel for absorption of methylene blue. *Carbohydr Polym* 153:34–46
- Vemmer M, AV Patel (2013). Review of encapsulation methods suitable for microbial biological control agents. *Biol Cont* 67:380–389
- Wijesinghe CJ, RW Wijeratnam, JKRR Samarasekara, RLC Wijesundera (2011). Development of a formulation of *Trichoderma asperellum* to control black rot disease on pineapple caused by *Thielaviopsis paradoxa*. *Crop Prot* 30:300–306
- Wu Z, Y He, L Chen, Y Han, C Li (2014). Characterization of *Raoultella planticola* Rs-2 microcapsule prepared with a blend of alginate and starch and its release behaviour. *Carbohydr Polym* 110:259–267
- Zohar-Perez C, I Chet, A Nussinovitch (2004). Irregular textural features of dried alginate-filler beads. *Food Hydrocoll* 18:249–258